

1 **Responses to Reviewers:**

2 **Reviewer 1:**

3 We thank the reviewer again for his/her careful reading of the manuscript and helpful comments.
4 We have revised the manuscript following the suggestions as is described below.

5 The authors made great efforts of revising the manuscript. However, the paper is still not
6 well written, and the conclusions were not convincingly supported by the data and method.
7 This is really an interesting scientific issue. I think there is still considerable more work
8 necessary to get the manuscript ready for publication at ACP. My major concerns are as
9 follows:

10 (1) The whole manuscript is based on the assumption that the co-occurrence of high ozone
11 and PM2.5 is under high HONO concentration. This assumption is highly possible to be true,
12 but it is lack of supportive measurement data. The authors have valuable HONO
13 measurements at three mega-cities including Beijing, Shanghai and Xi'An shown in Figure 8.
14 Since ozone and PM2.5 are routine measurement air pollutants, I would recommend
15 including them into the plot as well. Also, in Figure 8, since the measurement time is
16 different, I do not think they are comparable. I recommend separating Figure 8 into three
17 subplots by including ozone and PM2.5, and each subplot is for each city. So that the
18 assumption should be more solid.

19 Thanks for the constructive suggestion. We have separated Fig. 8 to 3 subplots. Fig. 8a shows
20 the measured PM2.5 and O₃, along with the measured HONO in Beijing. Fig. 8b shows the
21 measured PM2.5 and O₃, along with the measured and calculated HONO in Shanghai. Fig.
22 8c shows the measured PM2.5 and O₃, along with the measured HONO in Xi'an. All figures
23 show that there were co-occurrences of high O₃ and PM2.5, from late spring to early fall,
24 along with high HONO concentrations. These figures make the assumption to be more solid.
25 We have added the corresponding text in the revised version.

26 (2) The authors still did not state the set up of the WRF-Chem simulation, e.g. the gas-phase
27 mechanism used in the model? The authors need to at least briefly explain why the HONO
28 calculated by WRF-Chem is much lower than the observation. I think the model only
29 consider the HONO source with NO+OH only right? Also, how could the authors compare one
30 WRF-Chem modeling result to observations at three different cities during three
31 measurement time periods? All of those statement and comparison are not rigorous. Please
32 revise.

33 To address the comments of the reviewer, we add more details regarding the chemical
34 scheme of the WRF-Chem (the version which we used). We adding that "The version of the
35 WRF-Chem model is based on the version developed by Grell et al. (2015), and is improved
36 mainly by Tie et al. (2007) and Li et al. (2011). The chemical mechanism chosen in this
37 version of WRF-Chem is the RADM2 (Regional Acid Deposition Model, version 2) gas-phase
38 chemical mechanism. For the calculation of HONO, only the gas-phase chemistry of
39 OH+NO is included to calculate HONO concentrations. As shown in Fig. 8, the calculated
40 HONO concentrations are significantly smaller than the measured HONO values in eastern
41 China, suggesting that in addition to the gas-reaction, there are missing HONO sources
42 (surface sources or others). Because these missing sources are not fully understood and large
43 uncertainty is remained, in the following calculation, we compare the OH concentrations
44 due to both calculated HONO (without the missing sources) and the measured HONO
45 concentrations to illustrate the importance of these missing sources for the production of OH
46 radicals and to suggest that further study to better understand the missing sources is an
47 urgent scientific issue".

48 (3) Some conclusions and rationales are not rigorous. For example:

58
59 Line 278-279: Unless the authors show the error bars, this conclusion is not solid.
60 **We revise this statement**
61
62 Line 281-287: see my major concern (1).
63 **According to the reviewer's suggestion, we make 3 subplots (see answer 1)**
64
65 Line 289-295: If it is possible, it would be very helpful to include ozone measurement into
66 Figure 9 as well.
67 **Following the reviewer's comment, we add O3 measurement in Fig. 9.**
68
69 (4) The literature is not cited properly:
70 Line 100-102: the mixed regime for ozone formation is missed in the statement.
71 **Added.**
72
73 Line 130: Shi et al. (2015) never talked about "several potential HONO sources, including
74 surface emissions, conversion of NO 2 at the ocean surface, etc., and adding these sources
75 can improve the calculated HONO concentrations." These conclusions are from Zhang et al.
76 (2016).
77 **Corrected.**
78
79 Line 266: see my comments above, wrong citation.
80 **Corrected.**
81
82 (5) The paper is not very well written and organized. There are numerous typos and
83 grammar errors. Please carefully review the whole manuscript and revise them accordingly.
84 I listed some as follows, but not limited to:
85
86 Line 35: only "fall"? It seems the authors mentioned both "late spring and fall" in the
87 manuscript?
88 **Corrected. Changed to "from late spring to early fall" in all manuscript.**
89
90 Line 56: here is "spring and fall"? Please be consistent through the whole manuscript.
91 **Corrected.**
92
93 Line 99: grammar error - "... are becomes ..." Please revise.
94 **Corrected.**
95
96 Line 121: is it just "fall" or "late spring and fall"? Please be consistent through the whole.
97 **Corrected.**
98
99 Line 145 and 219: two section 2? Please revise.
100 **Corrected. Also for the following numbers of sections.**
101
102 Line 174-176: the sentence is redundant. Consider the following:
103 "The heavy aerosol concentrations play important roles to reduce solar radiation, causing
104 the reduction of O3 formation."
105 **Thanks. The sentence is changed according to the suggestion of the reviewer.**
106
107 Line 176: there is no Fig. 3a. Please indicate the upper panel as (a) in the plot or in the figure
108 capital.
109 **Corrected.**
110
111 Line 187: now the seasons include "late spring, summer, and early fall" instead of "late
112 spring and fall". I am very confused. Please be consistent about the seasons through the
113 whole manuscript.

114 Thanks for point out this typo. We checked all text, and changed to a consistent word "from
115 late spring to early fall".
116
117 Line 204-205: the sentence is redundant. Consider the following:
118 "both PM2.5 and O3 are severe air pollutants in eastern China."
119 Thanks. The sentence is changed according to the suggestion of the reviewer.
120
121 Line 207-217: Good!
122
123 Line 219 and Line 145: two section 2? Please revise.
124 Corrected.
125
126 Line 225: you mean "the surface solar radiation", not "the surface of solar radiation" right?
127 Corrected.
128
129 Line 236-237: "It can be expressed as"
130 Corrected.
131
132 Line 297-298: the sentence is redundant. Consider the following:
133 "the high HONO concentrations in daytime become a significant source of OH radicals."
134 Thanks. The sentence is changed according to the suggestion of the reviewer.
135
136 Line 339: it is "P2" not "P1" right?
137 Corrected.
138
139 Line 363 and Line 380: two section 3.3.
140 Corrected.
141
142 Line 384: "Figure 10 shows the OH concentrations in September and December"? What does
143 this mean? I thought Figure 10 shows a sensitivity study of OH production P using measured
144 and modeled HONO. Do I understand this correctly? Please revise.
145 Sorry. It should be Fig. 13 not Fig. 10. Corrected.
146
147 Line 412-413: "a double peak of PM2.5 and O3"? It sounds like for each pollutant, there is a
148 double peak. You mean "a co-occurrence of high PM2.5 and O3 concentrations"?
149 Thanks. We change this sentence to "a co-occurrence of high PM2.5 and O3 in some cases"
150
151 Line 413 and 432: only "fall" season?
152 Corrected.
153
154 Line 440: Delete "Because"
155 Corrected.
156
157
158
159
160
161
162
163
164
165

Ozone enhancement due to photo-disassocation of nitrous acid in eastern China

Xuexi Tie^{1,2}, Xin Long^{1,5}, Guohui Li¹, Shuyu Zhao¹, Junji Cao¹, Jianming Xu^{3,4}

¹ KЛАСР, SKLLQG, Institute of Earth Environment, Chinese Academy of Sciences, Xi'an 710061, China

²Center for Excellence in Urban Atmospheric Environment, Institute of Urban Environment, Chinese Academy of Sciences, Xiamen 361021, China

³ Shanghai Meteorological Service, Shanghai, 200030, China

⁴Shanghai Key Laboratory of Meteorology and Health, Shanghai, 200030, China

⁵School of Environment Science and Engineering, Southern University of Science and Technology, Shenzhen 518055, China

Correspondence to: XueXi Tie (tiexx@ieecas.cn) or

193 **Abstract**

194 PM_{2.5}, a particulate matter with a diameter of 2.5 micrometers or less, is one of the
195 major components of the air pollution in eastern China. In the past few years, China's
196 government made strong efforts to reduce the PM_{2.5} pollutions. However, another
197 important pollutant (ozone) becomes an important problem in eastern China. Ozone
198 (O₃) is produced by photochemistry, which requires solar radiation for the formation
199 of O₃. Under heavy PM_{2.5} pollution, the solar radiation is often depressed, and the
200 photochemical production of O₃ is prohibited. This study shows that during late
201 spring and early fall in eastern China, under heavy PM_{2.5} pollutions, there were often
202 strong O₃ photochemical productions, causing a co-occurrence of high PM_{2.5} and O₃
203 concentrations. This co-occurrence of high PM_{2.5} and O₃ is un-usual and is the main
204 focus of this study. Recent measurements show that there were often high HONO
205 surface concentrations in major Chinese mega cities, especially during daytime, with
206 maximum concentrations ranging from 0.5 to 2 ppbv. It is also interesting to note that
207 the high HONO concentrations were occurred during high aerosol concentration
208 periods, suggesting that there were additional HONO surface sources in eastern China.
209 Under the high daytime HONO concentrations, HONO can be photo-dissociated to be
210 OH radicals, which enhance the photochemical production of O₃. In order to study the
211 above scientific issues, a radiative transfer model (TUV; Tropospheric
212 Ultraviolet-Visible) is used in this study, and a chemical steady state model is
213 established to calculate OH radical concentrations. The calculations show that by
214 including the OH production of the photo-dissociated of HONO, the calculated OH
215 concentrations are significantly higher than the values without including this
216 production. For example, by including HONO production, the maximum of OH
217 concentration under the high aerosol condition (AOD=2.5) is similar to the value
218 under low aerosol condition (AOD=0.25) in the no-HONO case. This result suggests
219 that even under the high aerosol condition, the chemical oxidizing process for O₃
220 production can occurred, which explain the co-occurrence of high PM_{2.5} and high O₃
221 in late spring and early fall seasons in eastern China. However, the O₃ concentrations
222 were not significantly affected by the appearance of HONO in winter. This study
223 shows that the seasonal variation of solar radiation plays important roles for
224 controlling the OH production in winter. Because the solar radiation is in a very low
225 level in winter, adding the photolysis of HONO has smaller effect in winter than in

226 fall, and OH remains low values by including the HONO production term. This study
227 provides some important scientific highlights to better understand the O₃ pollutions in
228 eastern China.

229

230 **Keywords; High PM_{2.5} and O₃, eastern China, HONO photolysis**

231

232

233

234

235

236

237 **1. Introduction**

238

239 Currently, China is undergoing a rapid economic development, resulting in a higher
240 demand for energy and greater use of fossil fuels. As a result, the high emissions of
241 pollutants produce heavy pollutions in mega cities of eastern China, such as Beijing
242 and Shanghai. For example, in the city of Shanghai (a largest mega city in China), the
243 urban and economical developments of the city are very rapid. During 1990 to 2015,
244 the population increased from 13.3 to 24.1 million. The number of automobiles
245 increased from 0.2 million (1993) to 2.0 million (2011). The rapid growing population
246 and energy usage caused a rapid increase in the emissions of pollutants, leading to
247 severe air pollution problems in these mega cities (Zhang et al., 2006; Geng et al.,
248 2007; Deng et al., 2008).

249

250 Measurements, such as satellite observations have revealed much higher aerosol
251 pollution in eastern China than in eastern US (Tie et al., 2006). The high aerosol
252 pollution causes a wide range of environmental consequences. According to a study
253 by Tie et al. (2009a), exposure to extremely high particle concentrations leads to a
254 great increase of lung cancer cases. High PM (particular matter) concentrations also
255 significantly reduce the range of visibility in China's mega cities (Deng et al., 2008).
256 According to a recent study, the high aerosol pollution causes important effects on the
257 crop (rice and wheat) production in eastern China (Tie et al., 2016).

258

259 In the troposphere, ozone formation is resulted from a complicated chemical process,
260 and requires ozone precursors, such as VOCs (volatile organic carbons) and NO_x =
261 NO + NO₂ (nitrogen oxides) (Sillman, 1995). As the increase in industrial activity and
262 number of automobiles, the precursors of ozone (O₃) and the global budget of
263 oxidization are also significantly increased (Huang et al., 2017; Huang et al., 2018).

264 As a result, O₃ pollution becomes a serious pollution problem in Shanghai and other
265 Chinese mega cities (Geng et al., 2010; Tie 2009b; Tie et al., 2015). The effects on O₃
266 production rate can be characterized as either NO_x-sensitive or VOC-sensitive
267 conditions. For the city areas, O₃ production is generally VOC-sensitive, while in the
268 remote area, O₃ production is generally NO_x-sensitive in eastern China (Sillman,
269 1995; Zhang et al., 2003; Lei et al., 2004; Tie et al., 2013). Thus, better understanding

Xuexi Tie 8/9/2019 11:01 AM

Deleted: s are

Xuexi Tie 8/9/2019 11:00 AM

Deleted: s

Xuexi Tie 8/9/2019 3:35 PM

Formatted: Subscript

Xuexi Tie 8/9/2019 3:35 PM

Formatted: Subscript

272 the trends of O₃ precursors (VOCs, NO_x) is important to determine the O₃ trends in
273 Shanghai (as well as many large cities in China).

274 In the past few years, China's government made strong efforts to reduce the PM_{2.5}
275 pollutions. However, another important pollutant (O₃) becomes an important problem
276 in eastern China. Several studies regarding the O₃ formation are previously studied in
277 Shanghai. For example, Geng et al. (2007; 2008) study the relationship between O₃
278 precursors (NO_x and VOCs) for the ozone formation in Shanghai. Tie et al. (2009)
279 study the short-term variability of O₃ in Shanghai. Their study suggested that in
280 addition to the ozone precursors, meteorological conditions, such as regional transport,
281 have also strong impacts on the ozone concentrations. During September 2009, a
282 major field experiment (the MIRAGE-Shanghai) was conducted in Shanghai, and
283 multiply chemical species were measured during the experiment. The summary of the
284 measurements by Tie et al (2013) suggests that the ozone formation in Shanghai is
285 under VOC-sensitive condition. However, if the emission ration of NO_x/VOCs
286 reduces to a lower value (0.1-0.2), the ozone formation in Shanghai will switch from
287 VOC-sensitive condition to NO_x-sensitive condition.

288 Despite of some progresses have been made for the ozone formation in mega cities in
289 China, it is still lack of study of ozone development in large cities of China. For
290 example, this study shows that during late spring and early fall in eastern China, under
291 heavy PM_{2.5} pollutions, there were often strong O₃ chemical productions, causing the
292 co-occurrence of high PM_{2.5} and O₃ concentrations. Under heavy aerosol condition,
293 the solar radiation is depressed, significantly reducing the photochemical production
294 of O₃. This co-occurrence of high PM_{2.5} and O₃ is an unusual and is the focus of this
295 study. He and Carmichael (1999) suggest that aerosol particles can enhance the
296 scattering of solar radiation, enhancing the flux density inside the boundary layer.
297 Recent measurements also show that there were often high HONO concentrations in
298 major Chinese mega cities, especially during daytime, with maximum concentrations
299 ranging from 0.5 to 2 ppbv (Huang et al., 2017). Zhang et al. (2016) suggest that there
300 are several potential HONO sources, including surface emissions, conversion of NO₂
301 at the ocean surface, etc., and adding these sources can improve the calculated HONO
302 concentrations. It is also interesting to note that the high HONO surface
303 concentrations were occurred during high aerosol concentration periods, suggesting

Xuexi Tie 8/9/2019 10:54 AM

Deleted: Shi

Xuexi Tie 8/9/2019 10:55 AM

Deleted: 5

306 that there are additional HONO surface sources in eastern China. Under the high
307 daytime HONO concentrations, HONO can be photo-dissociated to be OH radicals,
308 which enhance the photochemical production of O₃.

309

310 The paper is organized as follows: in Section 2, we describe the measurement of O₃
311 and PM_{2.5}. In Section 3, we describe the calculation of photo-dissociated rate of
312 HONO and a steady state model for the calculation of OH, and the causes of high O₃
313 production under the heavy aerosol condition. Section 4 shows a brief conclusion of
314 the results.

315

316 **2. Measurements of O₃ and PM_{2.5}**

317

318 There are long-term measurements in Eastern China by Chinese Environment
319 Protection Agency (CEPA) for monitoring the air quality in China. In eastern China,
320 especially in the capital city of China (Beijing), there are often heavy air pollutions,
321 especially for fine particular matter (PM_{2.5} – the radius of particle being less than 2.5
322 um). Figure 1 shows the measurement sites in Beijing, in which the measured
323 concentrations of PM_{2.5} and O₃ are used to the analysis. In the region, the air
324 pollutions were very heavy, especially in winter (Long et al., 2016; Tie et al., 2017).
325 The previous studies suggested that the both aerosol and O₃ pollutions became the
326 major pollutants in the region (Li et al., 2017).

327

328 Figure 2 shows the daily averaged concentrations of PM_{2.5} and O₃ in the Beijing
329 region in 2015. The daily averaged concentrations show that there were strong daily
330 and seasonal variations for both the concentrations of PM_{2.5} and O₃. Despite the daily
331 variation, the concentrations of PM_{2.5} existed a strong seasonal variation. For example,
332 there were very high concentrations during winter, with maximum of ~300 $\mu\text{g}/\text{m}^3$.
333 While in summer, the maximum concentrations reduced to ~150 $\mu\text{g}/\text{m}^3$. The seasonal
334 variability of O₃ concentrations were opposite with the PM_{2.5} concentrations, with
335 lower concentrations in winter (< 50 $\mu\text{g}/\text{m}^3$) and higher concentrations in summer (>
336 150 $\mu\text{g}/\text{m}^3$). These seasonal variations of PM_{2.5} and O₃ have been studied by previous
337 studies (Tie and Cao, 2017; Li et al., 2017). Their results suggest that the winter high
338 PM_{2.5} concentrations were resulted from the combination of both the high emissions

339 (heating season in the Beijing region), and poor meteorological ventilation conditions,
340 such as lower PBL (Planetary Boundary Layer) height (Quan et al., 2013; Tie et al.
341 2015). According to the photochemical theory of O₃ formation, the summer high and
342 winter low O₃ concentrations are mainly due to seasonal variation of the solar
343 radiation (Seinfeld, J. H. and Pandis, 2006).

344

345 The heavy aerosol concentrations play important roles to reduce solar radiation,
346 causing the reduction of O₃ formation. (Bian et al., 2007). As we show in Fig. 3
347 (upper panel), during wintertime, the O₃ concentrations were strong anti-correlated
348 with the PM_{2.5} concentrations, suggesting that the reduction of solar radiation by
349 aerosol particles have important impact on the reduction of O₃ concentrations. Figure
350 3 (upper panel), also shows that the relationship between O₃ and PM_{2.5} was not
351 linearly related. For example, when the concentrations of PM_{2.5} were less than 100
352 $\mu\text{g}/\text{m}^3$, O₃ concentrations rapidly decreased with the increase of PM_{2.5} concentrations.
353 In contrast, when the concentrations of PM_{2.5} were greater than 100 $\mu\text{g}/\text{m}^3$, O₃
354 concentrations slowly decreased with the increase of PM_{2.5} concentrations. This is
355 consistent with the result of Bian et al (2007).

356

357 It is interesting to note that from late spring to early fall periods, the correlation
358 between PM_{2.5} and O₃ concentrations was positive relationship compared to the
359 negative relationship in winter (see Fig. 3 (lower panel)). This result suggests that O₃
360 production was high during the heavy haze period, despite the solar radiation was
361 greatly depressed. In order to clearly display this unusual event, we illustrate diurnal
362 variations of PM_{2.5} and O₃, and NO₂ during a fall period (from Oct. 5 to Oct. 6, 2015).
363 Figure 4 shows that during this period (as a case study), the PM_{2.5} concentrations were
364 very high, ranging from 150 to 320 $\mu\text{g}/\text{m}^3$. Under such high aerosol condition, the
365 solar radiation should be significantly reduced, and O₃ photochemical production
366 would be reduced. However, the diurnal variation of O₃ was unexpectedly strong,
367 with high noontime concentration of $>220 \mu\text{g}/\text{m}^3$ and very low nighttime
368 concentration of $\sim 25 \mu\text{g}/\text{m}^3$. This strong diurnal variation was due to the
369 photochemical activity, which suggested that during relatively low solar conditions,
370 the photochemical activities of O₃ production was high. According to the theory of the
371 O₃ chemical production, the high O₃ production is related to high oxidant of OH
372 (Seinfeld and Pandis, 2006), which should not be occurred during lower solar

Xuexi Tie 8/9/2019 11:07 AM

Formatted: Font:Times New Roman, 12 pt

Xuexi Tie 8/9/2019 11:07 AM

Deleted: In addition to the seasonal variation of solar radiation, the heavy aerosol concentrations play important roles to reduce solar radiation, causing the reduction of O₃ formation

Xuexi Tie 8/9/2019 3:36 PM

Formatted: Font:Times New Roman, 12 pt, Subscript

Xuexi Tie 8/9/2019 11:07 AM

Formatted: Font:Times New Roman, 12 pt

Xuexi Tie 8/9/2019 11:10 AM

Deleted: a

Xuexi Tie 8/9/2019 11:11 AM

Deleted: a

Xuexi Tie 8/9/2019 11:22 AM

Deleted: during

Xuexi Tie 8/9/2019 11:22 AM

Deleted: ,

Xuexi Tie 8/9/2019 11:22 AM

Deleted: summer, and

Xuexi Tie 8/9/2019 11:12 AM

Deleted: b

384 radiation. This result brings important issue for air pollution control strategy, because
385 | both PM_{2.5} and O₃ are severe air pollutants in eastern China.

387 To clearly understand the effect of the high aerosol concentrations on solar radiation,
388 we investigate the meteorological conditions, such as cloud covers, relation humidity
389 (RH), and solar radiation during the period of the case study (see Figs. 5 and 6).
390 Figure 5 shows that the cloud condition was close to the cloud free condition, but
391 there was a very heavy aerosol layer in the Beijing region, suggesting that cloud cover
392 played a minor role in the reduction of the solar radiation. The measured RH values
393 (not shown) were generally higher than 60%, with a maximum of 95% during the
394 period. As a result, the high aerosol concentrations accompanied by high RH produced
395 important effects on solar radiation. As shown in Fig. 6, the daytime averaged solar
396 radiation was significantly reduced (about 40% reduction in Oct. 5-6 period compared
397 with the value of Oct. 8).

398

399 | **3. Method**

400 In order to better understand the O₃ chemical production occurred in heavy aerosol
401 condition in eastern China, the possible O₃ production in such condition is discussed.
402 Ozone photochemical production (P[O₃]) is strongly related to the amount of OH
403 radicals (Chameides et al., 1999). According to the traditional theory, the amount of
404 surface OH radicals is proportional to the surface solar radiation, which is represented
405 by

406

$$408 \quad [OH] = P[HOx]/L[HOx]^* \quad (R-1)$$

409

410 Where [OH] represents the concentration of hydroxyl radicals (#/cm³); HOx
411 represents the concentration of HO₂ + OH (#/cm³); P[HOx] represents the
412 photochemical production of HOx (#/cm³/s); and L[HOx]^* (1/s) represents the
413 photochemical destruction of HOx, which is normalized by the concentrations of OH.

414

415 The major process for the photochemical production of P[HOx] is through the O₃
416 photolysis and follows by the reaction with atmospheric water vapor. It can be
417 expressed as,

Xuexi Tie 8/9/2019 11:26 AM

Deleted: the

Xuexi Tie 8/9/2019 11:26 AM

Formatted: Font:Times New Roman, 12 pt

Xuexi Tie 8/9/2019 11:26 AM

Formatted: Font:Times New Roman, 12 pt, Subscript

Xuexi Tie 8/9/2019 11:26 AM

Formatted: Font:Times New Roman, 12 pt

Xuexi Tie 8/9/2019 11:26 AM

Formatted: Font:Times New Roman, 12 pt, Subscript

Xuexi Tie 8/9/2019 11:26 AM

Formatted: Font:Times New Roman, 12 pt

Xuexi Tie 8/9/2019 11:26 AM

Deleted: both air pollutants (high PM_{2.5} and O₃) were important air pollution problems in eastern China.

Xuexi Tie 8/9/2019 11:03 AM

Deleted: 2

Xuexi Tie 8/9/2019 11:29 AM

Formatted: Subscript

Xuexi Tie 8/9/2019 11:30 AM

Deleted: e of

Xuexi Tie 8/9/2019 11:31 AM

Deleted: by

425 $P[\text{HOx}] = J_1[\text{O}_3]/(k_1 \times \text{am}) \times 2.0 \times k_2[\text{H}_2\text{O}] = P_1[\text{HOx}]$ (R-2)

426
427 Where J_1 represents the photolysis of $\text{O}_3 + h\nu \rightarrow \text{O}^1\text{D}$; k_1 represents the reaction rate
428 of $\text{O}^1\text{D} + \text{am} \rightarrow \text{O}^3\text{P}$; and k_2 represents the reaction rate of $\text{O}^1\text{D} + \text{H}_2\text{O} \rightarrow 2\text{OH}$. As
429 we can see, this HOx production is proportional to the magnitude of solar radiation
430 (J_1), and J_1 is the O_3 photolysis with the solar radiation. Figure 7 shows the
431 relationship between the values of J_1 and aerosol concentrations in October at
432 middle-latitude calculated by the TUV model (Madronich and Flocke, 1999). This
433 result suggests that under the high aerosol concentrations ($\text{AOD} = 2.5$), the J_1 value is
434 strongly depressed, resulting in significant reduction of OH concentrations and O_3
435 production. For example, the maximum J_1 value is about 2.7×10^{-5} (1/s) with lower
436 aerosol values ($\text{AOD} = 0.25$). According to the previous study, the surface $\text{PM}_{2.5}$
437 concentrations were generally smaller than $50 \mu\text{g}/\text{m}^3$ with this AOD value (Tie et al.,
438 2017). However, when the AOD value increase to 2.5 (the $\text{PM}_{2.5}$ concentrations are
439 generally $>100 \mu\text{g}/\text{m}^3$), the maximum J_1 value rapidly decreases to about 6×10^{-6} (1/s),
440 which is about 450% reduction compared to the value with $\text{AOD}=0.25$. This study
441 suggests that under high $\text{PM}_{2.5}$ concentrations ($>100 \mu\text{g}/\text{m}^3$), the photochemical
442 production of OH ($P[\text{HOx}]$) is rapidly decreased, leading to low OH concentrations,
443 which cannot initiate the high oxidation of O_3 production. As a result, the high O_3
444 production shown in Fig. 4 cannot be explained. Other sources for O_3 oxidation are
445 needed to explain this result.

446
447 Recent studies show that the HONO concentrations are high in eastern China (Huang
448 et al., 2017). Because under high solar radiation, the photolysis rate of HONO is very
449 high, resulting in very low HONO concentrations in daytime (Seinfeld and Pandis,
450 2006). These measured high HONO concentrations are explained by their studies.
451 One of the explanations is that there are high surface HONO sources during daytime,
452 which produces high HONO concentrations (Huang et al., 2017). Zhang et al. (2016)
453 suggest that there are several potential HONO sources, including surface emissions,
454 conversion of NO_2 at the ocean surface, etc. Zhang et al. (2016) parameterized these
455 potential HONO sources in the WRF-Chem model, and the calculated HONO
456 concentrations are increased in the WRF-Chem model.

Xuexi Tie 8/9/2019 10:56 AM

Deleted: Shi

Xuexi Tie 8/9/2019 10:56 AM

Deleted: 5

The version of the WRF-Chem model is based on the version developed by Grell et al. (2015), and is improved mainly by Tie et al. (2017) and Li et al. (2011). The chemical mechanism chosen in this version of WRF-Chem is the RADM2 (Regional Acid Deposition Model, version 2) gas-phase chemical mechanism. For the calculation of HONO, only the gas-phase chemistry of OH+NO is included to calculate HONO concentrations. As shown in Fig. 8, the calculated HONO concentrations are significantly smaller than the measured HONO values in eastern China, suggesting that in addition to the gas-reaction, there are missing HONO sources (surface sources or others). Because these missing sources are not fully understood and large uncertainty is remained, in the following calculation, we compare the OH concentrations due to both calculated HONO (without the missing sources) and the measured HONO concentrations to illustrate the importance of these missing sources for the production of OH radicals and to suggest that further study to better understand the missing sources is an urgent scientific issue.

Figure 8 shows the measured HONO concentrations in three large cities in China (Shanghai, Xi'an, and Beijing) during fall and winter. It also shows the corresponding PM_{2.5} and O₃ in the 3 cities (i.e., Fig. 8a for Beijing, Fig. 8b for Shanghai, and Fig. 8c for Xian). It shows that the measured HONO concentrations were high, ranging from sub-ppbv to a few ppbv, with higher values during morning, and lower values in daytime. The co-occurrences of high PM_{2.5} and O₃ happened in the 3 cities. As a result, we think that the high HONO is a common event in large cities in eastern China, especially in daytime. This high HONO is also measured by previous studies (Zhang et al. 2016; Huang et al. 2017). In this study, we make an assumption that the co-occurrence between O₃ and PM_{2.5} occurred under high HONO concentrations. We note that using this assumption may result in some uncertainties in estimating the effect of HONO on OH. For example, using the measured HONO in Xi'an and Beijing could produce 1-2 times higher OH production by photolysis of HONO than the result by using the data from Shanghai. In this case, we use the measured HONO from Shanghai to avoid the over estimate of the HONO effect, which can be considered as a low-limit estimation.

It is also interesting to note that the high HONO concentrations were occurred during high aerosol concentration periods. Figure 9 illustrates that when the $PM_{2.5}$

Xuexi Tie 8/9/2019 10:28 AM
Formatted: Font:(Default) Times New Roman, 12 pt
Xuexi Tie 8/9/2019 10:28 AM
Formatted: Font:(Default) Times New Roman
Xuexi Tie 8/9/2019 10:28 AM
Formatted: Font:(Default) Times New Roman, 12 pt
Xuexi Tie 8/9/2019 10:28 AM
Formatted: Font:(Default) Times New Roman
Xuexi Tie 8/9/2019 10:28 AM
Formatted: Font:(Default) Times New Roman, 12 pt
Xuexi Tie 8/9/2019 10:28 AM
Formatted: Font:(Default) Times New Roman
Xuexi Tie 8/9/2019 10:28 AM
Formatted: Font:(Default) Times New Roman, 12 pt
Xuexi Tie 8/9/2019 10:28 AM
Formatted: Font:(Default) Times New Roman
Xuexi Tie 8/9/2019 10:28 AM
Formatted: Font:(Default) Times New Roman, 12 pt
Xuexi Tie 8/9/2019 10:28 AM
Formatted: Font:(Default) Times New Roman
Xuexi Tie 8/9/2019 10:28 AM
Formatted: Font:(Default) Times New Roman, 12 pt
Xuexi Tie 8/9/2019 10:30 AM
Deleted: In our calculation, we only use the classical gas-phase chemistry to calculate HONO concentrations, and to illustrate that the importance of these missing sources for the production of OH radicals. Adding these missing sources (there are not fully understand and remain a large uncertainty) could be a very important future work. ¹
Xuexi Tie 8/8/2019 10:36 AM
Formatted: Subscript
Xuexi Tie 8/8/2019 10:36 AM
Formatted: Subscript
Xuexi Tie 8/8/2019 10:38 AM
Deleted: a maximum concentration of 2.3 ppbv
Xuexi Tie 8/8/2019 10:38 AM
Deleted: about 0.5-1.0 ppbv

505 concentrations increased to 70-80 $\mu\text{g}/\text{m}^3$, and the HONO concentrations enhanced to
506 1.4-18 ppbv during September in Shanghai. This measured high HONO
507 concentrations were significantly higher than the calculated concentrations (shown in
508 Fig. 8), suggesting that some additional sources of HONO are needed. This result is
509 consistent with the HONO measurements in other Chinese cities (Huang et al. 2017).

510

511 The high HONO concentrations in daytime become a significant source of OH
512 radicals. As a result, the OH production rate ($P[\text{HOx}]$) can be written to the following
513 reactions.

514

$$P_2[\text{HOx}] = J_2 \times [\text{HONO}] \quad (\text{R-3})$$

$$P[\text{HOx}] = P_1[\text{HOx}] + P_2[\text{HOx}]$$

$$= J_1[\text{O}_3]/(k_1 \times \text{am}) \times 2.0 \times k_2[\text{H}_2\text{O}] + J_2 \times [\text{HONO}] \quad (\text{R-4})$$

518

519 Because the chemical lifetime of OH is less than second, OH concentrations can be
520 calculated according to equilibrium of chemical production and chemical loss. With
521 the both OH chemical production processes, the OH concentrations can be calculated
522 by the following equation (Seinfeld and Pandis, 2006).

523

$$P_1 + P_2 = L_1 + L_2$$

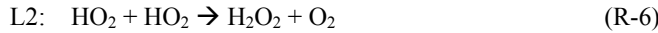
525

526 Where P_1 and P_2 are the major chemical productions, expressed in R-4, and L_1 and
527 L_2 are the major chemical loss of OH, and represent by

528



530



531

532 Under high NOx condition, such as in the large cities in eastern China, NOx
533 concentrations were often higher to 50 ppbv (as shown in Fig. 4). As a result, the L_1
534 term is larger than L_2 . The OH concentrations can be approximately expressed as

$$[\text{HO}] = \{J_1[\text{O}_3]/(k_1 \times \text{am}) \times 2.0 \times k_2[\text{H}_2\text{O}] + J_2 \times [\text{HONO}]\}/ \quad (\text{R-5})$$

535

536

753 Xuexi Tie 8/9/2019 11:33 AM
754 Formatted: Font:Times New Roman, 12
755 pt
756 Xuexi Tie 8/9/2019 11:33 AM
757 Deleted: Under the high HONO
758 concentrations in daytime, HONO can be
759 photolyzed to be OH, and become another
760 important process to produce OH.

753 Xuexi Tie 8/9/2019 3:40 PM
754 Deleted: Shanghai region
755 Xuexi Tie 8/9/2019 3:41 PM
756 Deleted: 5
757 Xuexi Tie 8/9/2019 3:40 PM
758 Deleted: ppbv (shown in Fig. 3),
759 Xuexi Tie 8/9/2019 3:41 PM
760 Deleted: by

547 Where k_3 is the reaction coefficient of $\text{OH} + \text{NO}_2 \rightarrow \text{HNO}_3$.

548

549 | 4. Result and analysis

550

551 | 4.1. OH productions in different HONO conditions

552

553 In order to quantify the individual effects of these two OH production terms (P1 and
554 P2) on the OH concentrations, the P1 and P2 are calculated under different daytime
555 HONO conditions (calculated low HONO and measured high HONO concentrations).
556 Figure 10 shows that under the low HONO condition, the P1 is significantly higher
557 than P2, and P2 has only minor contribution to the OH values. For example, the
558 maximum of P1 occurred at 13 pm, with a value of $65 \times 10^6 \text{#/cm}^3/\text{s}$. In contrast, the
559 maximum of P2 occurred at 10 am, with a value of $15 \times 10^6 \text{#/cm}^3/\text{s}$. However, under
560 high HONO condition, the P2 plays very important roles for the OH production. The
561 maximum of P2 occurred at 11 am, with a value of $350 \times 10^6 \text{#/cm}^3/\text{s}$, which is about
562 500% higher than the P1 value. It is important to note that this calculation is based on
563 the high aerosol condition (AOD = 2.5) in September. This result can explain the high
564 O₃ chemical production in Fig. 4.

565

566 | 4.2. OH in different aerosol conditions

567

568 In order to understand the effect of aerosol conditions, especially high aerosol
569 conditions, on the OH concentrations. Figure 11 shows the OH concentrations with
570 and without HONO production of OH. With including the HONO production (i.e.,
571 including P1 and P2), the calculated OH concentrations are significantly higher than
572 without including this production (i.e., only including P1). The both calculated OH
573 concentrations are rapidly changed with different levels of aerosol conditions. For
574 example, without HONO production, the maximum OH concentration is about
575 $7.5 \times 10^5 \text{#/cm}^3$ under low aerosol condition (AOD=0.25). In contrast, the maximum
576 OH concentration rapidly reduced to $1.5 \times 10^5 \text{#/cm}^3$ under high aerosol condition
577 (AOD=2.5), and further decreased to $1.0 \times 10^5 \text{#/cm}^3$ with the AOD value of 3.5. In
578 contrast, with including HONO production, the OH concentrations significantly
579 increased. Under higher aerosol condition (AOD=2.5), the maximum of OH
580 concentration is about $7.5 \times 10^5 \text{#/cm}^3$, which is the same value under low aerosol
581 condition in the no-HONO case. This result suggests that the measured high O₃

Xuexi Tie 8/9/2019 11:03 AM

Deleted: 3

Xuexi Tie 8/9/2019 11:03 AM

Deleted: 3

Xuexi Tie 8/9/2019 11:35 AM

Deleted: 1

Xuexi Tie 8/9/2019 11:03 AM

Deleted: 3

586 production occurred in the high aerosol condition is likely due to the high HONO
587 concentrations in Shanghai.

588

589 | **4.3. Effects of clouds**

590
591 Cloud cover can have very important impacts on the photolysis of HONO, which can
592 affect the effect of HONO on the OH radicals. The above calculations are based on
593 the cloud-free condition, with heavy aerosol concentration in the Beijing region. As
594 shown in Fig. 5, during the case study period (Oct 5 to 6, 2015) (see Fig. 4), the
595 weather map shows that the cloud-free condition, with heavy aerosol condition.

596

597 In order to understand the effects of cloud on the photolysis of HONO, we include
598 different cloud covers in the TUV model. The calculated results show in Fig. 12.
599 The results show that the thin cloud (with cloud cover in 2 km and cloud water of 10
600 g/m³), could reduce the photolysis rate of HONO by about 40%, but the HONO could
601 still remain important effects. However, with dense cloud condition (with cloud
602 covers at 2 and 3 km and cloud water of 50 10 g/m³), the photolysis rate of HONO
603 could reduce by 9-10 times by the cloud. In this case, adding photolysis rate of
604 HONO cannot produce important effect on OH radicals and the production of O₃.

605

606 | **4.4. OH in winter**

607
608 The measurement of O₃ also shows that the concentrations in winter were always low
609 (see Fig. 2), suggesting that the O₃ concentrations were not significantly affected by
610 the appearance of HONO. Figure 13 shows the OH concentrations in September and
611 December. It shows that under different aerosol conditions, OH concentrations in
612 December were very low compared with the values in September. Both the calculated
613 OH concentrations include the HONO production term. For example, under the
614 condition of AOD=2.5, the maximum OH is about 7.5×10^5 #/cm³ in September, while
615 it rapidly reduces to 1.5×10^5 #/cm³ in December. Under the condition of AOD=3.5,
616 the maximum OH is still maintaining to a relative high level (4.5×10^5 #/cm³) in
617 September. However, the maximum OH values are extremely low in December, with
618 maximum value of 0.5×10^5 #/cm³ in December. Because both the OH chemical
619 productions (P1 and P2) are strongly dependent upon solar radiation (see equation
620 R-4), the seasonal variation of solar radiation plays important roles for controlling the

Xuexi Tie 8/9/2019 11:03 AM

Deleted: 3

Xuexi Tie 8/9/2019 11:03 AM

Deleted: 3

Xuexi Tie 8/9/2019 11:36 AM

Deleted: 3

Xuexi Tie 8/9/2019 11:48 AM

Deleted: 0

625 OH production in winter (see Fig. 13). Because the solar radiation is in a very low
626 level in winter, adding the photolysis of HONO has smaller effect in winter than in
627 other seasons and OH remains low values by including the HONO production term.

Xuexi Tie 8/9/2019 12:03 PM
Deleted: fall,

629 Summary

631 Currently, China is undergoing a rapid economic development, resulting in a high
632 demand for energy, greater use of fossil fuels. As a result, the high emissions of
633 pollutants produce heavy aerosol pollutions (PM_{2.5}) in eastern China, such as in the
634 mega city of Beijing. The long-term measurements show that in addition to the heavy
635 aerosol pollution, the O₃ pollution becomes another major pollutants in the Beijing
636 region. The measured results show that there were very strong seasonal variation in
637 the concentrations of both PM_{2.5} and O₃ in the region. During winter, the seasonal
638 variability of O₃ concentrations were anti-correlated with the PM_{2.5} concentrations.

639 However, from late spring to early fall, the correlation between PM_{2.5} and O₃
640 concentrations was positive compared to the negative in winter. This result suggests
641 that during heavy aerosol condition (the solar radiation was depressed), the O₃
642 chemical production was still high, appearing a co-occurrence of high PM_{2.5} and O₃ in
643 some cases from late spring to early fall. This co-occurrence of high PM_{2.5} and O₃ is
644 the focus of this study. The results are highlighted as follows;

645
646 (1) There are high daytime HONO concentrations in major Chinese mega cities, such
647 as in Beijing and Shanghai. It is also interesting to note that the high HONO
648 concentrations were occurred during high aerosol concentration periods. Under
649 the high daytime HONO concentrations, HONO can be photo-dissociated to be
650 OH radicals, and becomes an important process to produce OH.

651 (2) With including the OH production of measured HONO concentrations, the
652 calculated OH concentrations are significantly higher than without including this
653 production. For example, without HONO production, the maximum OH
654 concentration is about 7.5×10^5 #/cm³ under low aerosol condition (AOD=0.25),
655 and rapidly reduced to 1.5×10^5 #/cm³ under high aerosol condition (AOD=2.5) in
656 September. In contrast, by including HONO production, the OH concentrations
657 significantly increased. For example, under higher aerosol condition (AOD=2.5),
658 the maximum of OH concentration is about 7.5×10^5 #/cm³, which is similar to the

Xuexi Tie 8/9/2019 11:15 AM
Deleted: during
Xuexi Tie 8/9/2019 11:15 AM
Deleted: and
Xuexi Tie 8/9/2019 11:17 AM
Deleted: 1 periods
Xuexi Tie 8/9/2019 11:57 AM
Formatted: Font:Times New Roman, 12 pt
Xuexi Tie 8/9/2019 11:57 AM
Formatted: Font:Times New Roman, 12 pt, Subscript
Xuexi Tie 8/9/2019 11:57 AM
Formatted: Font:Times New Roman, 12 pt
Xuexi Tie 8/9/2019 11:57 AM
Formatted: Font:Times New Roman, 12 pt, Subscript
Xuexi Tie 8/9/2019 11:58 AM
Formatted: Font:Times New Roman, 12 pt
Xuexi Tie 8/9/2019 11:57 AM
Deleted: a double peak of PM_{2.5} and O₃
Xuexi Tie 8/9/2019 11:17 AM
Deleted: during
Xuexi Tie 8/9/2019 11:17 AM
Deleted: period

666 value under low aerosol condition in the no-HONO case. This result suggests that
667 even under the high aerosol conditions, the chemical oxidizing process for O₃
668 production can be active. This result is likely for explaining the co-occurrence of
669 high PM_{2.5} and high O₃ from late spring to early in eastern China.

670 (3) The measurement of O₃ also shows that the concentrations in winter were always
671 low, suggesting that the O₃ concentrations were not significantly affected by the
672 appearance of HONO. The calculated result shows that the seasonal variation of
673 solar radiation plays important roles for controlling the OH production in winter.
674 Because the solar radiation is in a very low level in winter, adding the photolysis
675 of HONO has smaller effect in winter than in other seasons, and OH remains low
676 values by including the HONO production term.

677 In recent years, the PM_{2.5} pollutions are reduced due to the large control efforts by the
678 Chinese government, the O₃ pollutions become another severe pollution problem in
679 eastern China. This study is important, because it provides some important scientific
680 highlights to better understand the O₃ pollutions in eastern China.

681
682 **Data availability.** The data used in this paper can be provided upon request from
683 Xuexi Tie (tiexx@ieecas.cn).

684
685 **Author contributions.** XT came up with the original idea of investigating the
686 scientific issue. XT and JX designed the analysis method. XL, GL and SZ provided
687 the observational data and helped in discussion. XT prepared the manuscript with
688 contributions from all co-authors.

689
690 **Acknowledgement**
691 This work was supported by the National Natural Science Foundation of China
692 (NSFC) under Grant Nos. 41430424 and 41730108. The Authors thanks the supports
693 of Center for Excellence in Urban Atmospheric Environment, Institute of Urban
694 Environment, Chinese Academy of Sciences.

695
696

Xuexi Tie 8/9/2019 11:17 AM

Deleted: in

Xuexi Tie 8/9/2019 11:18 AM

Deleted: fall season

Xuexi Tie 8/9/2019 11:18 AM

Deleted: fall

Xuexi Tie 8/9/2019 11:59 AM

Deleted: Because i

701 **References**

702

703 Bian H., S.Q. Han, X. Tie, M.L. Shun, and A.X. Liu, Evidence of Impact of Aerosols
704 on Surface Ozone Concentration: A Case Study in Tianjin, China, *Atmos.*
705 *Environ.*, 41, 4672-4681, 2007.

706 Chameides, W. L., Fehsenfeld, F., Rodgers, M. O., Cardelino, C., Martines, J., Parrish,
707 D., Lonneman, W., Lawson, D. R., Ras-mussen, R. A., Zimmerman, P.,
708 Greenberg, J., Middleton, P., and Wang, T.: Ozone precursor relationships in the
709 ambient atmo- sphere, *J. Geophys. Res.*, 97, 6037-6055, 1992.

710 Deng X.J, X Tie, D. Wu, XJ Zhou, HB Tan, F. Li, C. Jiang, Long-term trend of
711 visibility and its characterizations in the Pearl River Delta Region (PRD), China,
712 *Atmos. Environ.*, 42, 1424-1435, 2008.

713

714 Geng, F.H., C.S., Zhao, X. Tang, GL. Lu, and X. Tie, Analysis of ozone and VOCs
715 measured in Shanghai: A case study, *Atmos. Environ.*, 41, 989-1001, 2007.

716 Geng, FH, CG Cai, X. Tie, Q. Yu, JL An, L. Peng, GQ Zhou, JM Xu, Analysis of
717 VOC emissions using PCA/APCS receptor model at city of Shanghai, China, *J.*
718 *Atmos. Chem.*, 62, 229-247, DOI :10.1007/s10874-010-9150-5, 2010.

719

720 Grell, G. A., Peckham, S. E., Schmitz, R., McKeen, S. A., Frost, G., Skamarock, W.
721 C., and Eder, B.: Fully coupled “online” chemistry within the WRF model, *Atmos.*
722 *Environ.*, 39, 6957– 6975, 2005.

723

724 He, S., & Carmichael, G. R. (1999). Sensitivity of photolysis rates and ozone pro-
725 duction in the troposphere to aerosol properties. *Journal of Geophysical Research: Atmospheres*, 104(D21), 26307-26324.

725

726 Huang, J.P, X. Y. Liu, C. Y. Li, L. Ding, H. P. Yu, The global oxygen budget and its
727 future projection. *Science Bull.* 63, 1180–1186, 2018.

728

729 Huang J., Y. Li, C. Fu, F. Chen, Q. Fu, A. Dai, M. Shinoda, Z. Ma, W. Guo, Z. Li, L.
730 Zhang, Y. Liu, H. Yu, Y. He, Y. Xie, X. Guan , M. Ji, L. Lin, S. Wang, H. Yan
731 and G. Wang, Dryland climate change recent progress and challenges. *Rev. of*
732 *Geophys.*, 55, 719-778, doi:10.1002/2016RG000550, 2017.

733

734 Huang, R. J., L. Yang, JJ Cao, QY Wang, X. Tie, et al., Concentration and sources of
735 atmospheric nitrous acid (HONO) at an urban site in Western China. *Sci. of Total*
736 *Environ.*, 593-594, 165-172, doi.org/10.1016/j.scitotenv.2017.02.166, 2017.

737

738 Lei, W., R. Zhang, X. Tie, P. Hess, Chemical characterization of ozone formation in
739 the Houston-Galveston area, *J. Geophys. Res.*, 109, doi:10.1029/2003JD004219,
740 2004.

741 Li, G., Bei, N., Tie, X., and Molina, L. T.: Aerosol effects on the photochemistry in
742 Mexico City during MCMA-2006/MILAGRO campaign, *Atmospheric Chemistry*
743 and Physics, 11, 5169–5182, 2011.

Xuexi Tie 8/9/2019 10:19 AM

Formatted: Font:(Default) Times New Roman, 12 pt

Xuexi Tie 8/9/2019 10:21 AM

Formatted: Font:(Default) Times New Roman, 12 pt

Xuexi Tie 8/9/2019 10:21 AM

Formatted: Font:(Default) Times New Roman

745 Li, G., Bei, N., Cao, J., Wu, J., Long, X., Feng, T., Dai, W., Liu, S., Zhang, Q., and
 746 Tie, X.: Widespread and persistent ozone pollution in eastern China during the
 747 non-winter season of 2015: observations and source attributions, *Atmos. Chem. Phys.*, 17, 2759-2774, doi:10.5194/acp-17-2759-2017, 2017.

749 Long, X., X. Tie, JJ Cao, RJ Huang, T. Feng, N. Li, SY Zhao, J. Tian, GH Li, Q.
 750 Zhang, Impact of crop field burning and mountains on heavy haze in the North
 751 China Plain: A case study, *Atmos. Chem. Phys.*, 16, 9675-9691,
 752 doi:10.5194/acp-16-9675-2016, 2016.

753 Madronich, S. & Flocke, S. in *Environmental Photochemistry 2 / 2L*, 1-26 (Springer
 754 Berlin Heidelberg, 1999)

755 Quan, J.N., Y. Gao, Q. Zhang, X. Tie*, JJ Cao, SQ Han, JW Meng, PF Chen, DL
 756 Zhao, Evolution of Planetary Boundary Layer under different weather conditions,
 757 and its impact on aerosol concentrations, *Particuology*, doi:
 758 10.1016/j.partic.2012.04.005, 2013.

759 Seinfeld, J. H. and Pandis, S. N.: *Atmospheric Chemistry and Physics: From Air
 760 Pollution to Climate Change*, 2nd Edn., John Wiley and Sons, New York, 2006.

761 Shi, C., Wang, S., Liu, R., Zhou, R., Li, D., Wang, W., ... & Zhou, B. (2015). A study
 762 of aerosol optical properties during ozone pollution episodes in 2013 over
 763 Shanghai, China. *Atmospheric Research*, 153, 235-249.

764 Sillman, S.: The use of NO_y, H₂O₂, and HNO₃ as indicators for
 765 ozone-NO_x-hydrocarbon sensitivity in urban locations, *J. Geo- phys. Res.*, 100,
 766 14175-14188, 1995.

767 Tie, X., G. Brasseur, C. Zhao, C. Granier, S. Massie, Y. Qin, P.C. Wang, GL Wang,
 768 PC, Yang100,, Chemical Characterization of Air Pollution in Eastern China and
 769 the Eastern United States, *Atmos. Environ.*, 40, 2607-2625, 2006.

770

771 Tie, X., Madronich, S., Li, G., Ying, Z., Zhang, R., Garcia, A., Taylor, J., and Liu, Y.:
 772 Characterizations of chemical oxidants in Mexico City: A regional chemical
 773 dynamical model (WRF-Chem) study, *Atmospheric Environment*, 41, 1989-2008,
 774 2007.

775 Tie, X., D. Wu, and G. Brasseur, Lung Cancer Mortality and Exposure to
 776 Atmospheric Aerosol Particles in Guangzhou, China, *Atmos. Environ.*, 43, 2375-
 777 2377, 2009a.

778 Tie, X., FH. Geng, L. Peng, W. Gao, and CS. Zhao, Measurement and modeling of O₃
 779 variability in Shanghai, China; Application of the WRF-Chem model, *Atmos.
 780 Environ.*, 43, 4289-4302, 2009b.

781 Tie, X., F. Geng, A. Guenther, J. Cao, J. Greenberg, R. Zhang, E. Apel, G. Li,
 782 A. Weinheimer, J. Chen, and C. Cai, Megacity impacts on regional ozone

Xuexi Tie 8/9/2019 3:27 PM

Deleted: .

Xuexi Tie 8/9/2019 3:27 PM

Formatted: Font:(Default) Times New Roman, 12 pt, Font color: Auto

Xuexi Tie 8/9/2019 3:27 PM

Formatted: Font:(Default) Times New Roman, 12 pt

Xuexi Tie 8/9/2019 3:27 PM

Formatted: Left, Indent: Left: 0",
 Hanging: 0.31", Space After: 12 pt, Line spacing: at least 15 pt, Don't adjust space
 between Latin and Asian text, Don't adjust space between Asian text and numbers

Xuexi Tie 8/9/2019 3:27 PM

Deleted: .

Xuexi Tie 8/9/2019 3:27 PM

Formatted: Font color: Black

785 formation: observations and WRF-Chem modeling for the MIRAGE-Shanghai
786 field campaign, *Atmos. Chem. Phys.*, 13, 5655-5669, doi:10.5194/acp-13-5655-2013, 2013.

788 Tie, X., Q. Zhang, H. He, JJ Cao, SQ Han, Y. Gao, X. Li, and XC Jia, A budget
789 analysis on the formation of haze in Beijing, *Atmos. Environ.*, 25-36, 2015.

790 Tie, X., RJ Huang, WT Dai, JJ Cao, X. Long, XL Su, SY Zhao, QY Wang, GH Li,
791 Effect of heavy haze and aerosol pollution on rice and wheat productions in China,
792 *Sci. Rep.* 6, 29612; doi: 10.1038/srep29612, 2016.

793 Tie, X., J.J. Cao, Understanding Variability of Haze in Eastern China, *J Fundam
794 Renewable Energy Appl.*, 7:6 DOI: 10.4172/2090-4541.100024, 2017.

795 Tie, X., R.J. Huang, J.J. Cao, Q. Zhang, Y.F. Cheng, H. Su, D. Chang, U. Pöschl, T.
796 Hoffmann, U. Dusek, G. H. Li, D. R. Worsnop, C. D. O'Dowd, Severe Pollution
797 in China Amplified by Atmospheric Moisture, *Sci. Rep.* 7: 15760 |
798 DOI:10.1038/s41598-017-15909-1, 2017.

799 Zhang, L., Wang, T., Zhang, Q., Zheng, J., Xu, Z., & Lv, M.. Potential sources of
800 nitrous acid (HONO) and their impacts on ozone: A WRF/Chem study in a
801 polluted subtropical region. *Journal of Geophysical Research: Atmospheres*,
802 121(7), 3645- 3662, 2016.

803

804 Zhang, R., X. Tie, and D. Bond, Impacts of Anthropogenic and Natural NO_x Sources
805 over the U.S. on Tropospheric Chemistry, *Proceedings of National Academic
806 Science USA*, 100, 1505-1509, 2003.

807 Zhang, Q., C. Zhao, X. Tie, Q. Wei ,G. Li, and C. Li, Characterizations of Aerosols
808 over the Beijing Region: A Case Study of Aircraft Measurements, 40,
809 4513-4527, *Atmos. Environ.*, 2006.

810

811

812 **Figure Caption**
813

814 **Fig. 1.** The geographic locations of the measurement sites in Beijing, in which the
815 measured concentrations of PM_{2.5} and O₃ are used to the analysis.
816

817 **Fig. 2.** The daily averaged concentrations of PM_{2.5} and O₃ in the Beijing region in
818 2015. The concentrations are averaged over all sites shown in Fig. 1. The blue lines
819 represent the PM_{2.5} concentrations ($\mu\text{g}/\text{m}^3$), and the red bars represent the O₃
820 concentrations ($\mu\text{g}/\text{m}^3$). The rectangles show some typical events during winter
821 (green), spring and fall (orange), and summer (red).
822

823 **Fig. 3.** The correlation between O₃ and PM_{2.5} concentrations during winter (upper
824 panel) and from late spring to early fall (lower panel). During winter, O₃
825 concentrations were strong anti-correlated with the PM_{2.5} concentrations. From late
826 spring to early fall, O₃ concentrations were correlated with the PM_{2.5} concentrations.
827

828 **Fig. 4.** The diurnal variations of PM_{2.5} (blue line) and O₃ (red line), and NO₂ (green
829 line) during a fall period (from Oct. 5 to Oct. 6, 2015). It shows that with high PM_{2.5}
830 condition, there was a strong O₃ diurnal variation.
831

832 **Fig. 5.** The cloud condition during the period of the case study (between Oct 5 and 6,
833 2015) in the Beijing region. The bright white color shows the cloud covers, and the
834 grey white shows the haze covers. The Beijing region was under the heavy haze
835 conditions during the period.
836

837 **Fig. 6.** The measured solar radiation (W/m^2) from Oct. 3 to Oct. 9, 2015 in Beijing.
838 The upper panel shows hourly values, and the lower panel shows the daytime
839 averaged values.
840

841 **Fig. 7.** The effect of aerosol levels with AOD = 0.25 (black line), AOD = 2.5 (red
842 line), AOD = 3.5 (blue line), and AOD = 4.0 (green line) on the O₃ photolysis
843 calculated by the TUV model in October at middle-latitude.
844

845 **Fig. 8a.** The measured HONO concentrations (ppbv) and the PM_{2.5} and O₃ daily
846 concentrations in Beijing. The upper panel shows the measured daily concentrations
847 of PM_{2.5} and O₃ as shown in Fig.2. The dark-red line was measured HONO in Beijing
848 from 1 to 27 January, 2014.
849

850 **Fig. 8b.** The measured HONO concentrations (ppbv) and the PM_{2.5} and O₃ daily
851 concentrations in Shanghai. The upper panel shows the measured daily concentrations
852 of PM_{2.5} and O₃ in 2015. The dark-red line was measured in Shanghai from 9 to 18
853 September, 2009. The green line was calculated by the WRF-Chem model.
854

855 **Fig. 8c.** The measured HONO concentrations (ppbv) and the PM_{2.5} and O₃ daily
856 concentrations in Xi'an. The upper panel shows the measured daily concentrations of
857 PM_{2.5} and O₃ in 2015. The red line was measured HONO in Xi'An from 24 July to
858 August 6, 2015.
859

860 **Fig. 9.** The measured HONO (upper left panel), PM_{2.5} concentrations (lower left
861 panel), and O₃ concentrations (upper right panel) in fall in Shanghai. It illustrates that
862

Xuexi Tie 8/9/2019 11:19 AM

Deleted: during

Xuexi Tie 8/9/2019 11:19 AM

Deleted: and

Xuexi Tie 8/9/2019 11:19 AM

Deleted:

Xuexi Tie 8/9/2019 11:20 AM

Deleted: During

Xuexi Tie 8/9/2019 11:20 AM

Deleted: and

Xuexi Tie 8/9/2019 11:20 AM

Formatted: Subscript

Xuexi Tie 8/8/2019 10:31 AM

Formatted: Font:12 pt

Xuexi Tie 8/8/2019 10:31 AM

Formatted: Font:12 pt

867 | the high HONO concentrations were corresponded with high PM_{2.5} concentrations.

868
869 **Fig. 10.** The calculated OH production P(HOx) (#/cm³/s) by using the model
870 calculated HONO (low concentrations) (in the upper panel) and by using the
871 measured HONO (high concentrations) (in the lower panel). The red bars represent
872 the calculation of the P1 term, and the red bars represent the calculation of the P2
873 term (OH production from HONO).

874
875 **Fig. 11.** The calculated OH concentrations (#/cm³) with (upper panel) and without
876 (lower panel) HONO production of OH, under different aerosol levels. Dark red
877 (AOD=0.25), red (AOD=2.5), red (AOD=3.5), and red (AOD=4.0).

878
879 **Fig. 12.** The effect of cloud cover on the photolysis rate of HONO (J[HONO]). The
880 blue, red, and green lines represent the cloud water vapor of 0 (cloud-free), 10 (g/m³ –
881 thin cloud), and 50 (g/m³ – thick cloud), respectively. The left panel (A) represents
882 the light aerosol condition, with AOD of 0.25, and the right panel (B) represents the
883 heavy aerosol condition, with AOD of 2.5.

884
885 **Fig. 13.** The calculated OH concentrations in September (blue bars) and December
886 (dark red bars), under different aerosol levels.

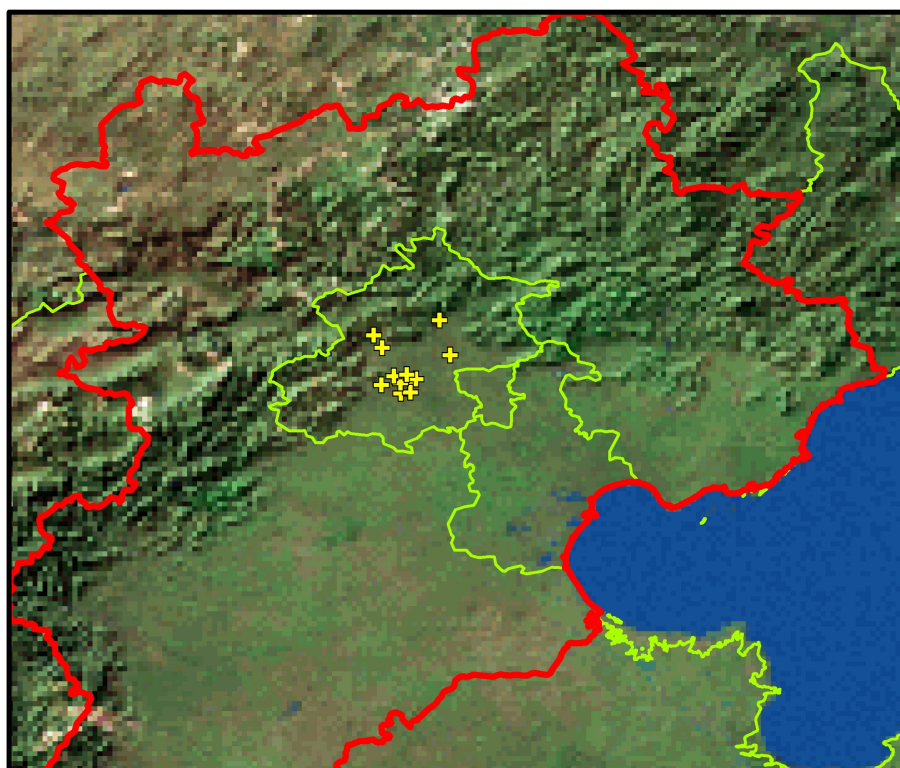
Xuexi Tie 8/8/2019 10:31 AM

Deleted: **Fig. 8.** The measured HONO concentrations (ppbv) in three large cities in China. The red line was measured in Xi'An from 24 July to August 6, 2015. The blue line was measured in Shanghai from 9 to 18 September, 2009. The dark-red line was measured in Beijing from 1 to 27 January, 2014. The green line is calculated by the WRF-Chem model. The measurement in fall of Shanghai is applied to the calculation for the OH production of HONO.

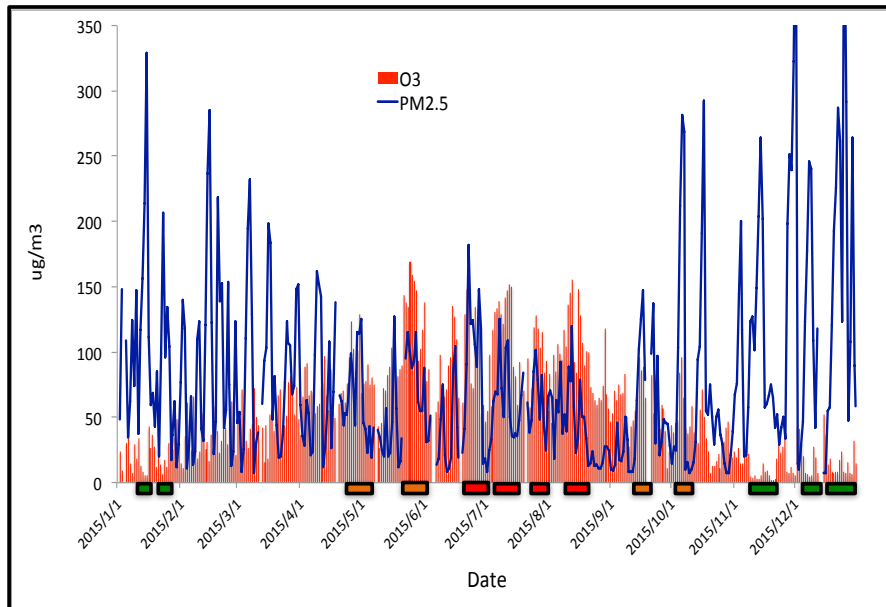
Xuexi Tie 8/8/2019 10:32 AM

Deleted: **Fig. 9.** The measured HONO (upper panel) and PM_{2.5} concentrations (lower panel) in fall in Shanghai. It illustrates that the high HONO concentrations were corresponded with high PM_{2.5} concentrations.

907 **Figures**
908



909
910
911 **Fig. 1.** The geographic locations of the measurement sites in Beijing, in which the measured
912 concentrations of $PM_{2.5}$ and O_3 are used to the analysis.
913



914
 915 **Fig. 2.** The daily averaged concentrations of PM_{2.5} and O₃ in the Beijing region in 2015. The
 916 concentrations are averaged over all sites shown in Fig. 1. The blue lines represent the PM_{2.5}
 917 concentrations ($\mu\text{g}/\text{m}^3$), and the red bars represent the O₃ concentrations ($\mu\text{g}/\text{m}^3$). The rectangles
 918 show some typical events during winter (green), spring and fall (orange), and summer (red).

919

920

921

922

923

924 |

925

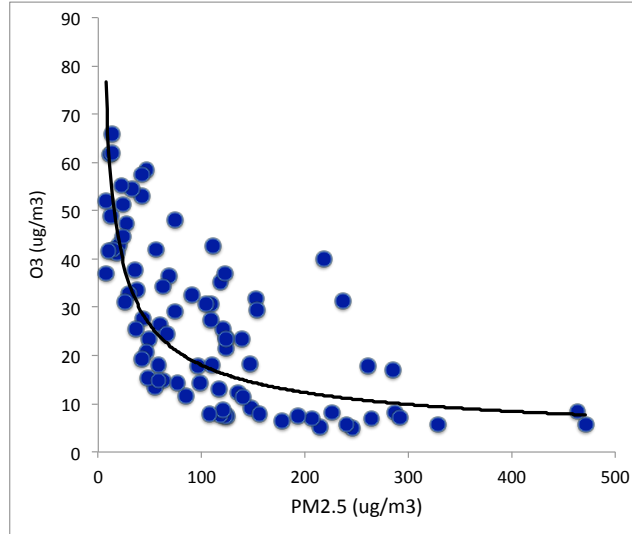
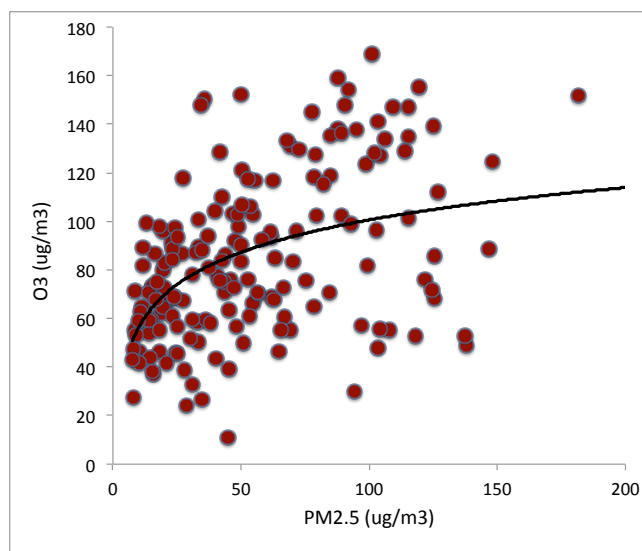
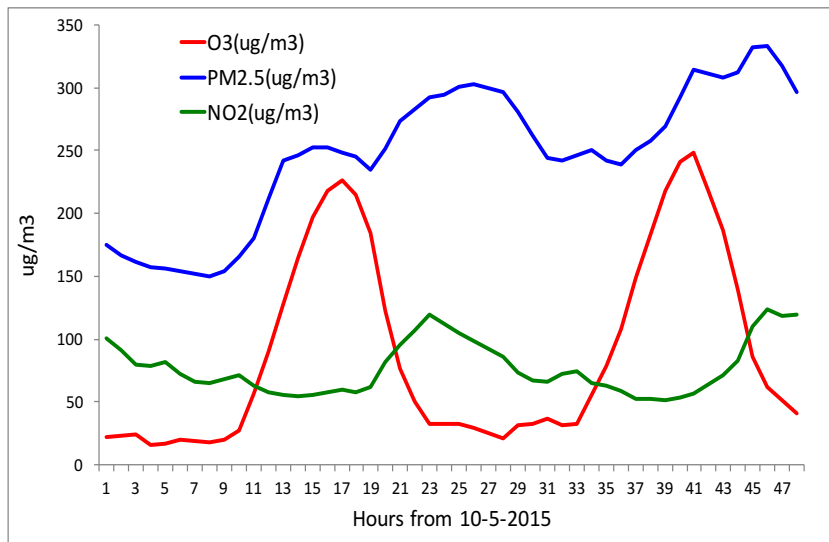
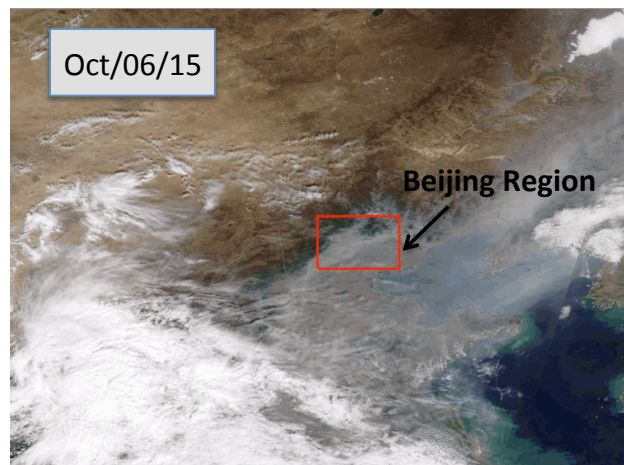
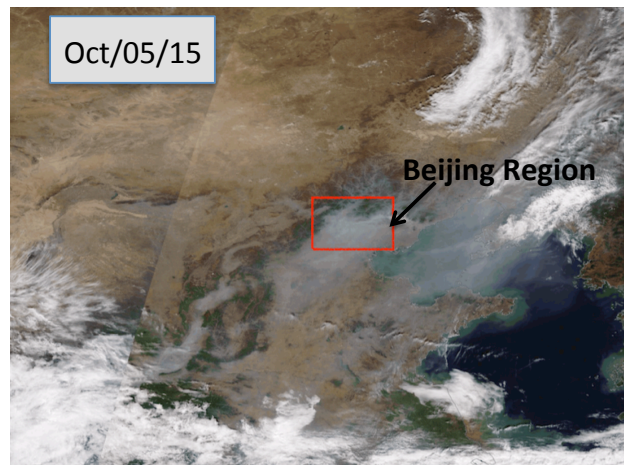
926
927928
929
930
931
932
933
934

Fig. 3. The correlation between O₃ and PM_{2.5} concentrations during winter (upper panel) and from late spring to early fall (lower panel). During winter, O₃ concentrations were strong anti-correlated with the PM_{2.5} concentrations. From late spring to early fall, O₃ concentrations were correlated with the PM_{2.5} concentrations.

Xuexi Tie 8/9/2019 3:44 PM
Deleted: during
Xuexi Tie 8/9/2019 3:44 PM
Deleted: and
Xuexi Tie 8/9/2019 3:45 PM
Deleted: During
Xuexi Tie 8/9/2019 3:45 PM
Deleted: and

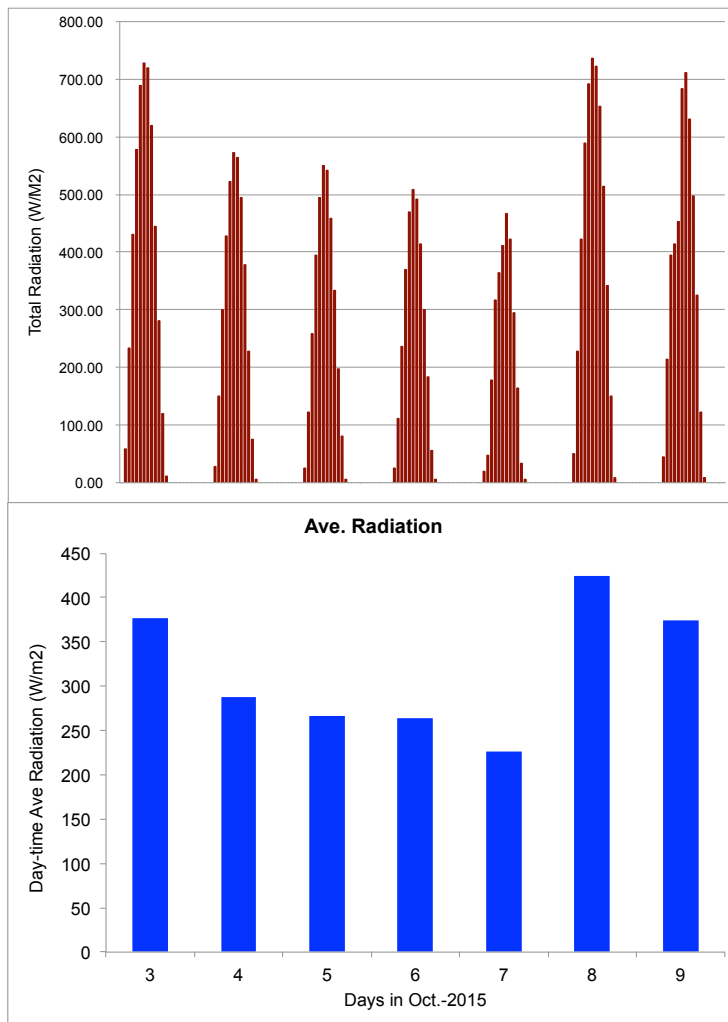


939
940
941 **Fig. 4.** The diurnal variations of PM_{2.5} (blue line) and O₃ (red line), and NO₂ (green line)
942 during a fall period (from Oct. 5 to Oct. 6, 2015). It shows that with high PM_{2.5} condition,
943 there was a strong O₃ diurnal variation.
944
945

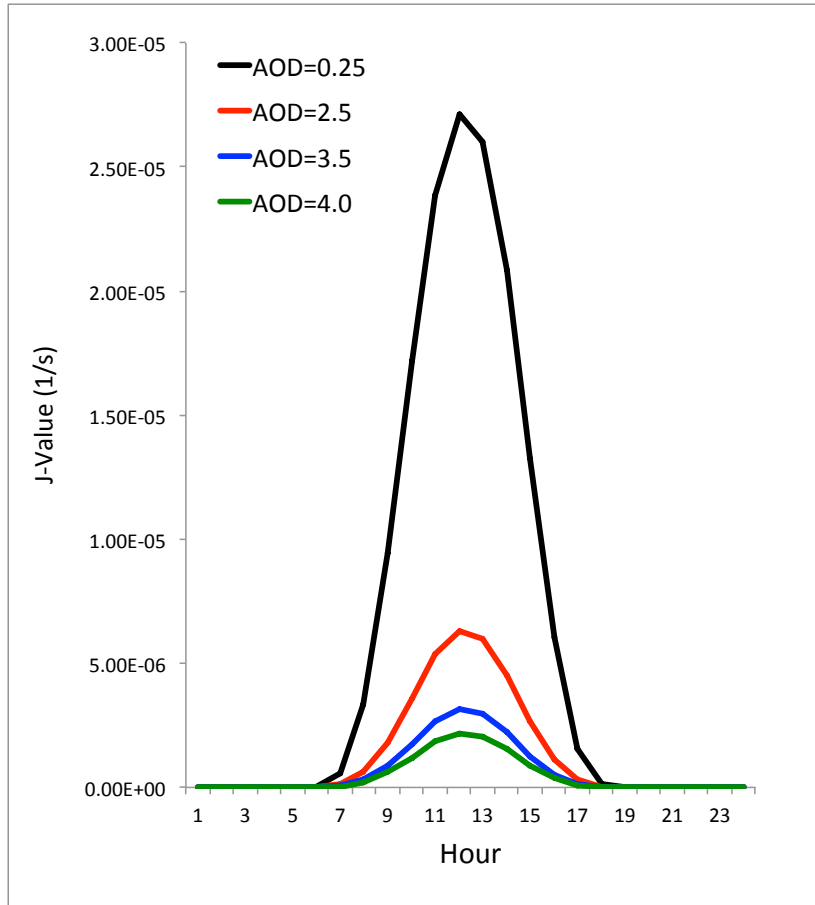


946
947
948
949
950

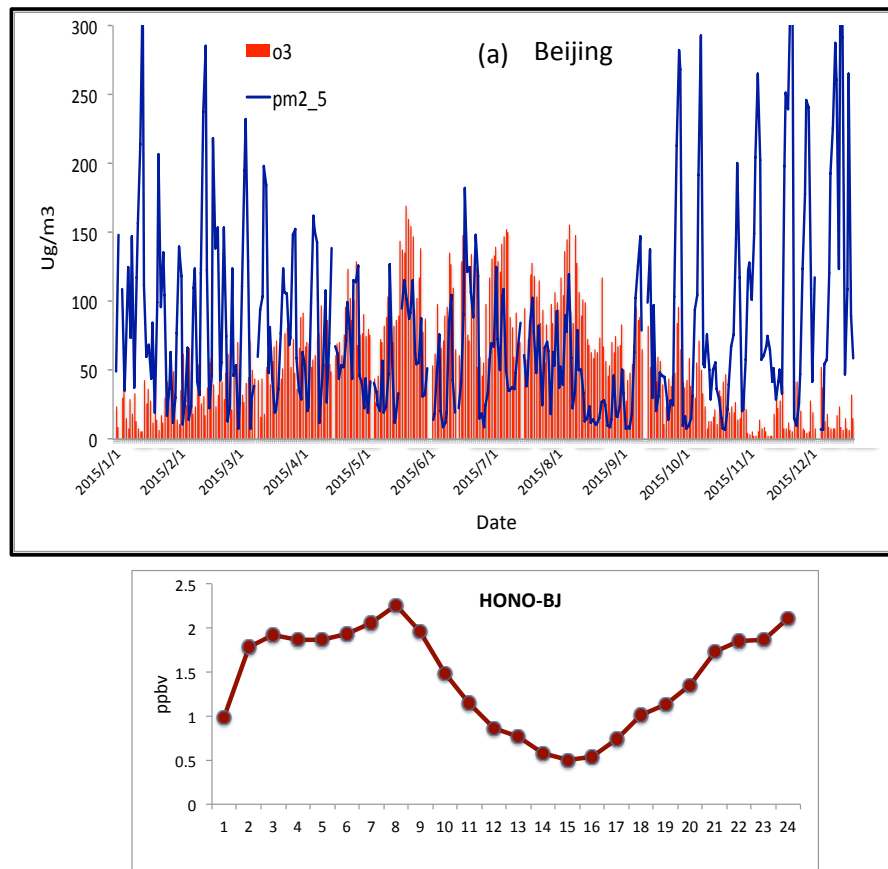
Fig. 5. The cloud condition during the period of the case study (between Oct 5 and 6, 2015 in the Beijing region. The bright white color shows the cloud covers, and the grey white shows the haze covers. The Beijing region is under the heavy haze conditions during the period.



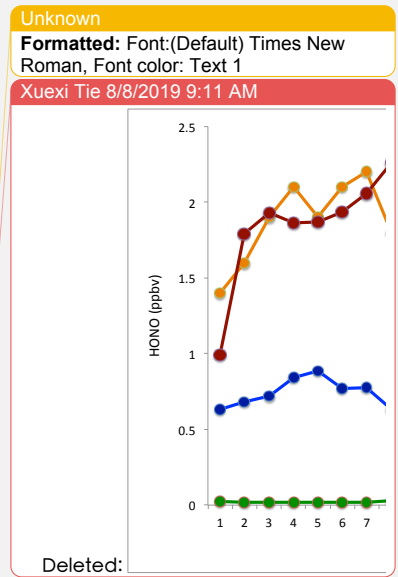
951
952 **Fig. 6.** The measured solar radiation (W/m²) from Oct. 3 to Oct. 9, 2015 in Beijing. The upper
953 panel shows hourly values, and the lower panel shows the daytime averaged values.
954
955



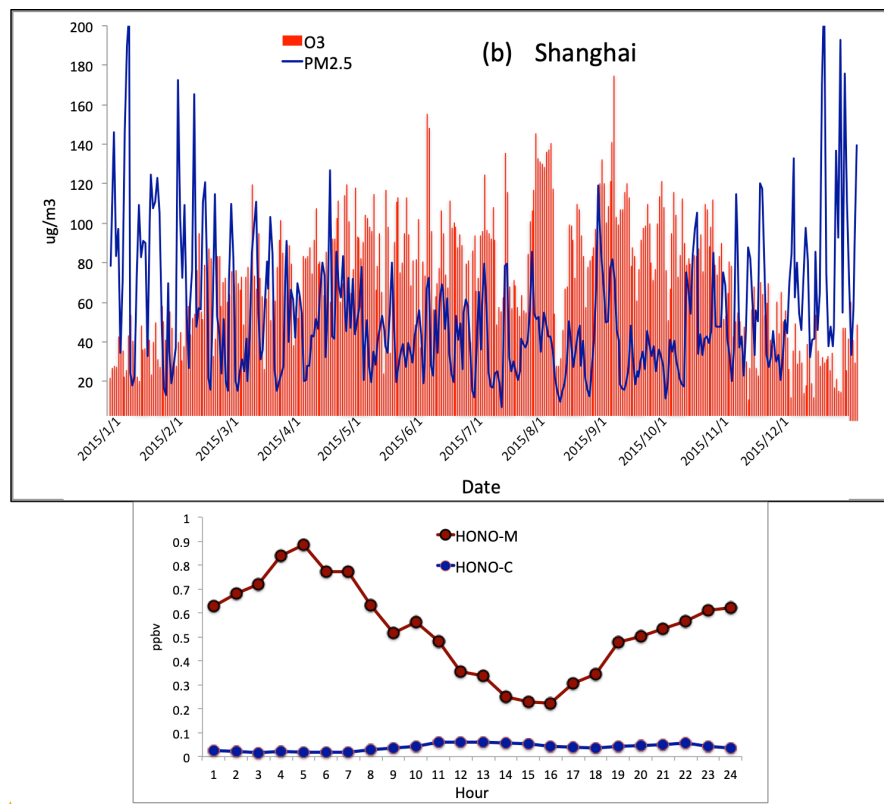
956
957
958 **Fig. 7.** The effect of aerosol levels with AOD = 0.25 (black line), AOD = 2.5 (red line),
959 AOD = 3.5 (blue line), and AOD = 4.0 (green line) on the O₃ photolysis calculated by
960 the TUV model in October at middle-latitude.
961



962
963
964
965 **Fig. 8a.** The measured HONO concentrations (ppbv) and the $\text{PM}_{2.5}$ and O_3 daily
966 concentrations in Beijing. The upper panel shows the measured daily concentrations of $\text{PM}_{2.5}$
967 and O_3 as shown in Fig.2. The dark-red line was measured HONO in Beijing from 1 to 27
968 January, 2014.
969



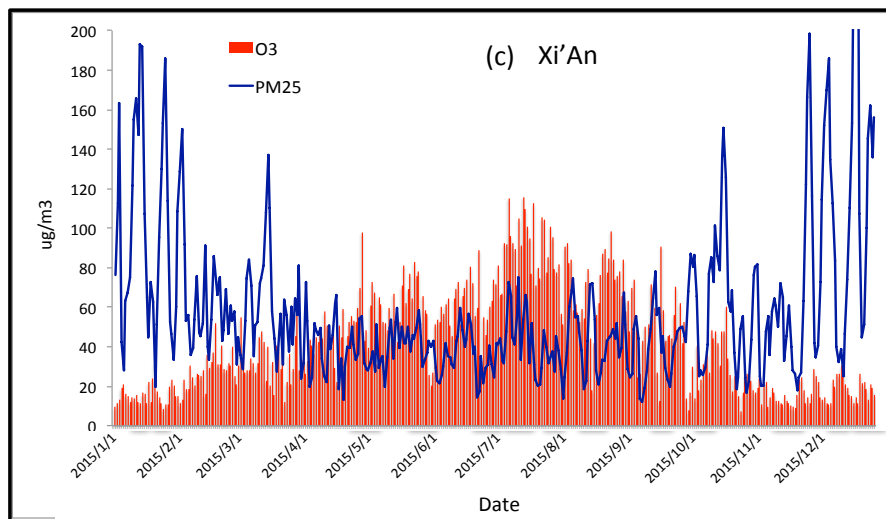
Xuexi Tie 8/8/2019 9:14 AM
Deleted: in
Xuexi Tie 8/8/2019 9:14 AM
Formatted: Subscript
Xuexi Tie 8/8/2019 9:14 AM
Formatted: Subscript
Xuexi Tie 8/8/2019 9:45 AM
Formatted: Subscript
Xuexi Tie 8/8/2019 9:45 AM
Formatted: Subscript
Xuexi Tie 8/8/2019 9:15 AM
Moved (insertion) [1]



Unknown

Formatted: Font:(Default) Times New Roman, 11 pt, Font color: Text 1

972
973
974
975 **Fig. 8b.** The measured HONO concentrations (ppbv) and the PM_{2.5} and O₃ daily
976 concentrations in Shanghai. The upper panel shows the measured daily concentrations of
977 PM_{2.5} and O₃ in 2015. The dark-red line was measured in Shanghai from 9 to 18 September,
978 2009. The green line was calculated by the WRF-Chem model.
979
980



981
982 Fig. 8c. The measured HONO concentrations (ppbv) and the PM_{2.5} and O₃ daily
983 concentrations in Xi'an. The upper panel shows the measured daily concentrations of PM_{2.5}
984 and O₃ in 2015. The red line was measured HONO in Xi'an from 24 July to August 6, 2015.
985
986
987
988
989
990
991

Unknown

Formatted: Font:(Default) Times New Roman, 11 pt, Font color: Text 1

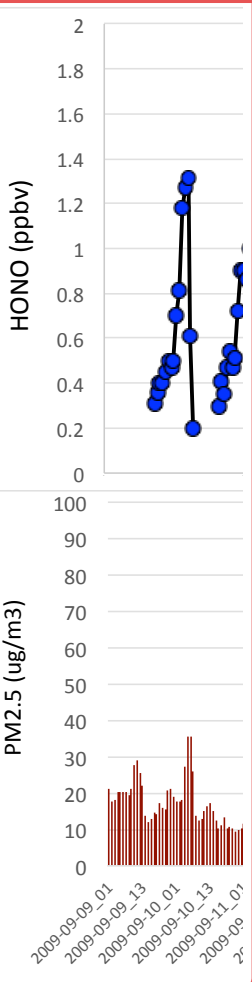
Xuexi Tie 8/8/2019 9:56 AM

Deleted: three large cities in China. The red line was measured in Xi'An from 24 July to August 6, 2015. The blue line was measured in Shanghai from 9 to 18 September, 2009. The dark-red line was measured in Beijing from 1 to 27 January, 2014. The green line is calculated by the WRF-Chem model. The measurement in fall of Shanghai is applied to the calculation for the OH production of HONO. [... \[1\]](#)

Xuexi Tie 8/8/2019 9:15 AM

Moved up [1]: The dark-red line was measured in Beijing from 1 to 27 January, 2014.

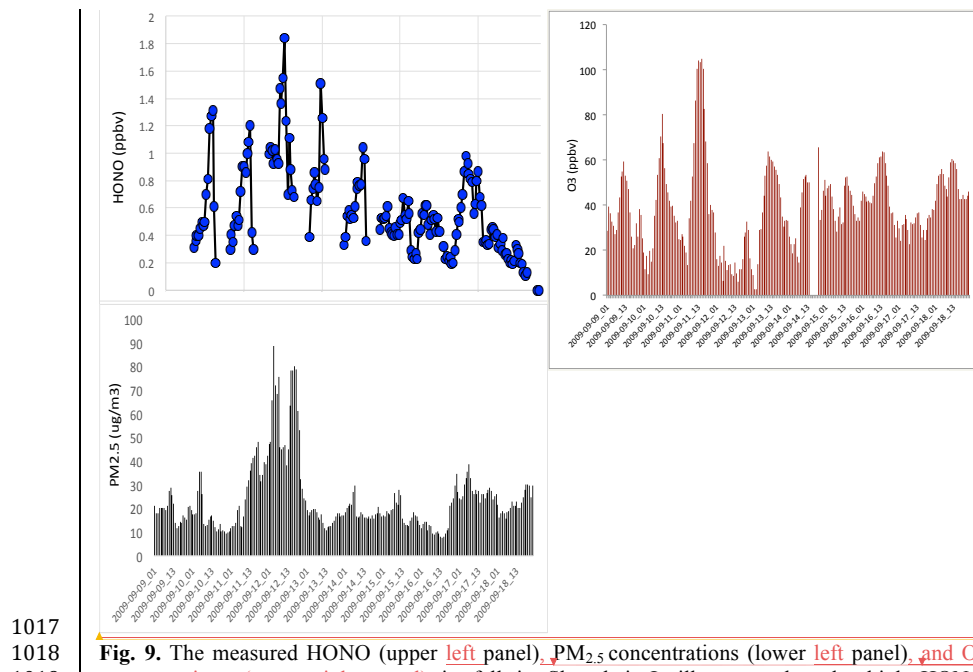
Xuexi Tie 8/8/2019 10:17 AM



Deleted:

Unknown

Formatted: Font:(Default) Times New Roman



1017
1018
1019
1020

Fig. 9. The measured HONO (upper left panel), PM_{2.5} concentrations (lower left panel), and O₃ concentrations (upper right panel) in fall in Shanghai. It illustrates that the high HONO concentrations were corresponded with high PM_{2.5} concentrations.

Unknown

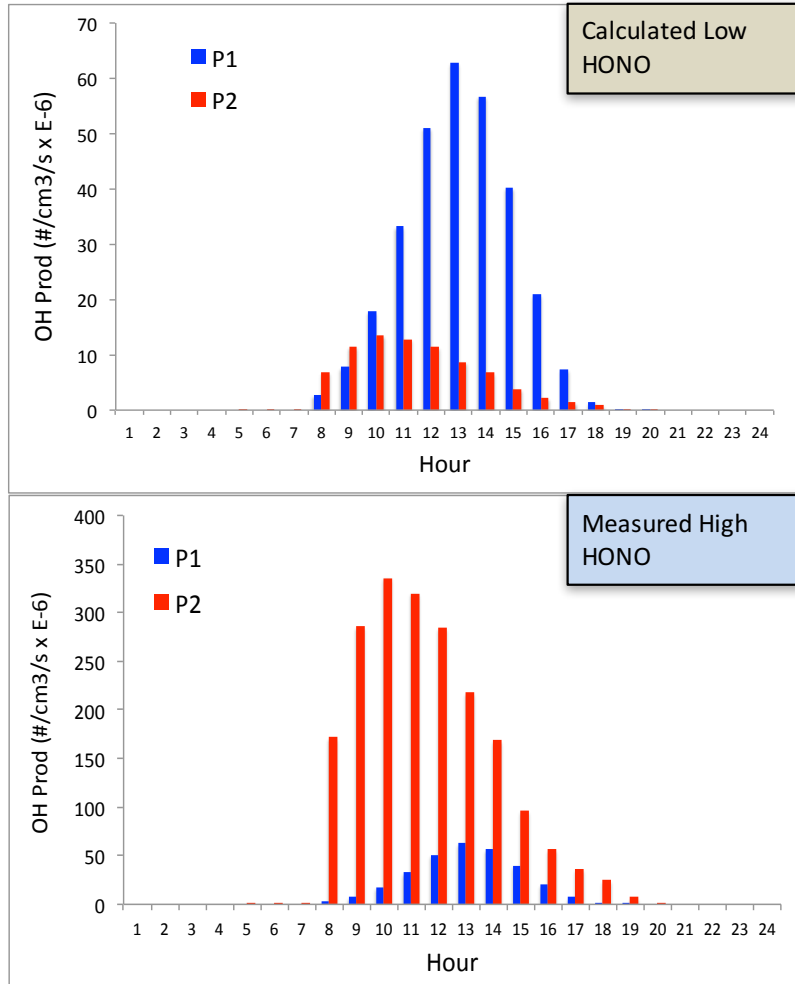
Formatted: Font:(Default) Times New Roman, Bold

Xuexi Tie 8/8/2019 10:17 AM

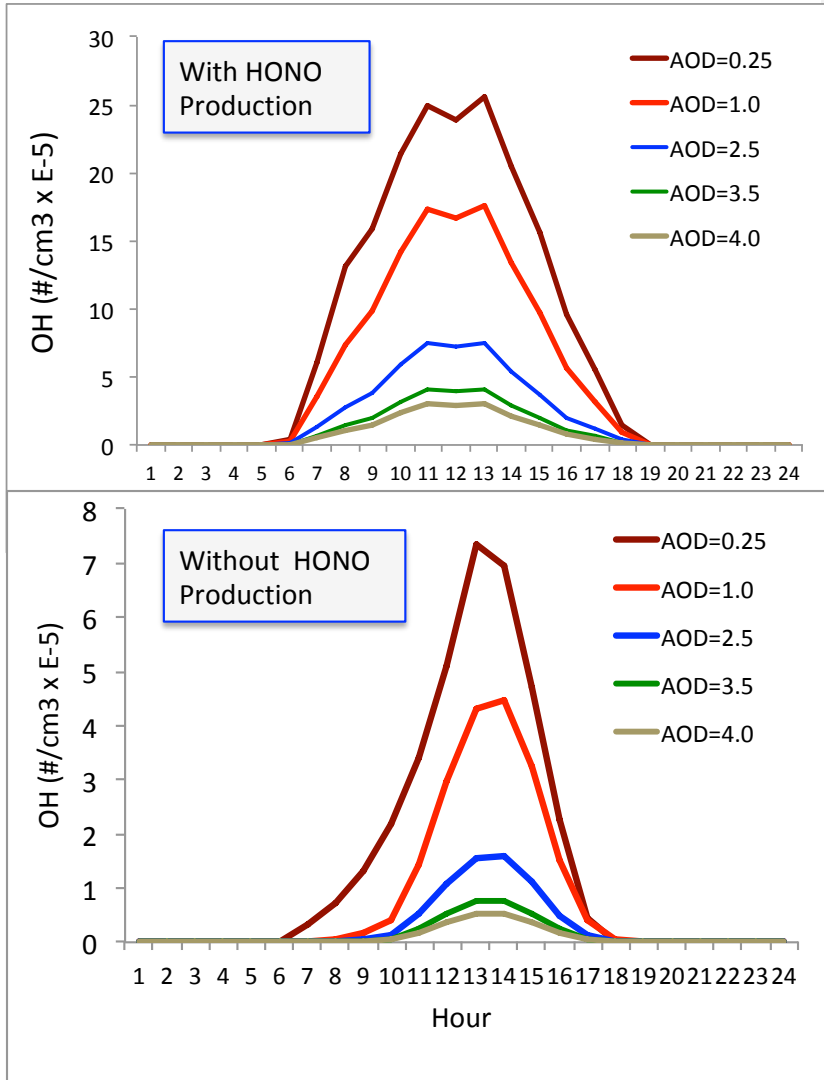
Deleted: and

Xuexi Tie 8/8/2019 10:18 AM

Deleted:

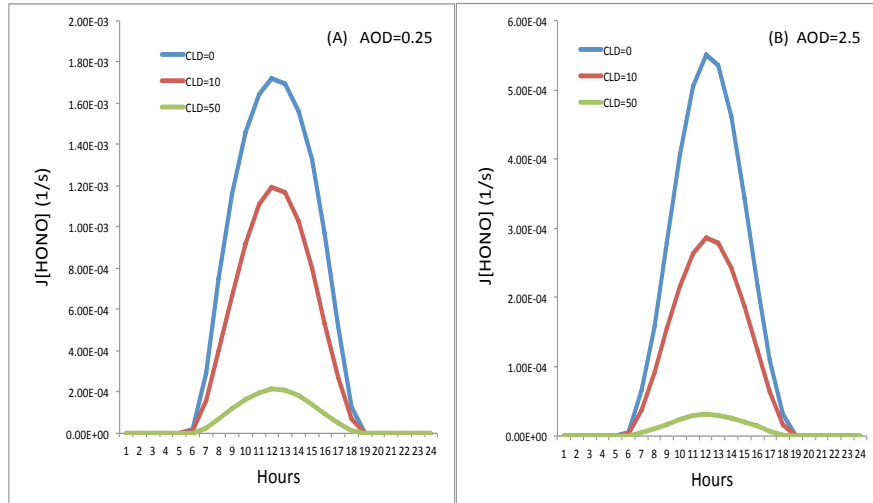


1023
1024
1025
1026
1027
1028
1029
Fig. 10. The calculated OH production $P(HO_x)$ ($\#/cm^3/s$) by using the model calculated
HONO (low concentrations) (in the upper panel) and by using the measured HONO
(high concentrations) (in the lower panel). The red bars represent the calculation of the
P1 term, and the red bars represent the calculation of the P2 term (OH production from
HONO).



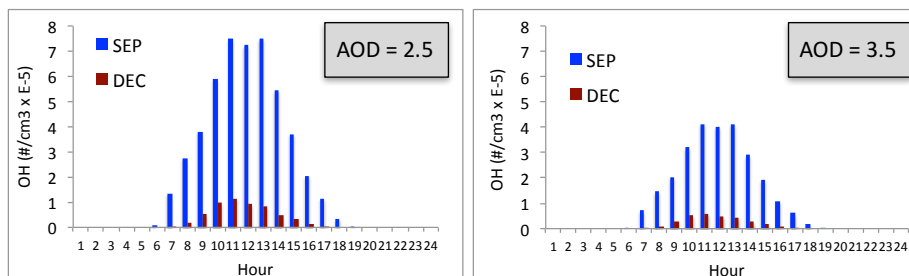
1030
1031
1032
1033
1034
1035
1036
1037

Fig. 11. The calculated OH concentrations ($\#/cm^3$) with (upper panel) and without (lower panel) HONO production of OH, under different aerosol levels. Dark red (AOD=0.25), red (AOD=2.5), red (AOD=3.5), and red (AOD=4.0).



1038
1039
1040 **Fig. 12.** The effect of cloud cover on the photolysis rate of HONO ($J[HONO]$). The blue, red, and
1041 green lines represent the cloud water vapor of 0 (g/m^3 – cloud-free), 10 (g/m^3 – thin cloud), and 50 (g/m^3
1042 – thick cloud), respectively. The left panel (A) represents the light aerosol condition, with AOD of
1043 0.25, and the right panel (B) represents the heavy aerosol condition, with AOD of 2.5.

1050
1051



1052
1053
1054
1055
1056

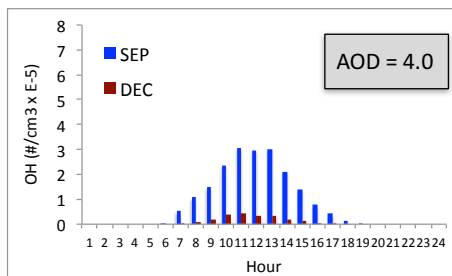


Fig. 13. The calculated OH concentrations in September (blue bars) and December (dark red bars), under different aerosol levels.